THE

PHYSICAL REVIEW

A journal of experimental and theoretical physics established by E. L. Nichols in 1893

SECOND SERIES, VOL. 75, No. 5 MARCH 1, 1949

Neutron-Proton and Neutron-Neutron Scattering at High Energies*

F. ROHRLICH** AND J. EISENSTEIN***

Lyman Laboratory of Physics, Harvard University, Cambridge, Massachusetts

(Received September 20, 1948)

The phase method and the Born approximation is used to calculate the cross sections of high energy neutrons scattered by protons and neutrons. Various exchange theories are considered for both, central and tensor forces of rectangular and Yukawa well shape.

For the tensor case the phase method leads to general formulas for the differential and total cross sections in terms of *real* phase shifts. The reality of the phase shifts is a direct consequence of the use of the asymptotic form of the eigenfunctions of the tensor force Hamiltonian. The differential cross section in this case also contains the "amounts of admixture" which measure the coupling of states of different orbital angular momentum which have the same total angular momentum and the same parity. The real phase shifts and the amounts of admixture are derived from a variational principle. The total cross sections thus obtained are within a few percent of the exact values. The Born approximation is not satisfactory at 100 Mev.

At this energy, tensor forces of a rectangular well shape with Rarita-Schwinger constants yield 0.2113, 0.1497, and 0.1271 barns for the *n-p* cross section, and 0.2566, 0.1381, and 0.0359 barns for the *n-n* cross section, in the neutral, charged, and symmetrical exchange theory, respectively. The observed *n-p* cross section at 90 Mev, 0.083±0.004 barns, agrees best with the theoretical value of ∼0.080 barns at 100 Mev, derived from a tensor interaction potential of equal amounts of neutral and charged exchange. It is concluded, however, that a Yukawa tensor potential of the symmetrical exchange type can be in agreement with the experiments, if relativistic corrections of the *n-p* cross section at 100 Mev are negative and of the order of 5–10 percent. The differential cross section needs considerably larger corrections unless a different tensor force range is used.

INTRODUCTION

THE phenomenological theories of nuclear forces could be compared until recently only with scattering data up to about 10 Mev. Neutron-proton and neutron-neutron scattering in this energy range is practically spherically symmetrical. No conclusion could, therefore, be reached about the exchange character of nuclear forces. Similarly, it was possible to fit the observed data with central and with tensor forces, and with a variety of different potential well shapes.[1] Recently, Sleator[2] measured the total *n-p* cross section at energies between 6 and 22 Mev. He found that six different theories are in fair agreement with the experiments at least on some part of the energy range, but that only the charged and the symmetrical tensor theory fit within the whole range considered. Proton-proton scattering experiments[3] at 14.5 Mev show a negative *P*-wave contribution to the angular distribution which indicates exchange forces. Neu-

* This work is based on parts of the theses submitted by the authors to the Graduate School of Arts and Sciences, Harvard University, in partial fulfilment of the requirements for the degree of Doctor of Philosophy.

** Now at the Institute for Advanced Study, Princeton, New Jersey.

*** National Research Council Predoctoral Fellow. Now at the University of Wisconsin, Madison, Wisconsin.

[1] D. Bohm and C. Richman, Phys. Rev. 71, 567 (1947).

[2] W. Sleator, Phys. Rev. 72, 207 (1947).

[3] Wilson, Lofgren, Richardson, Wright, and Shankland, Phys. Rev. 71, 560 and 72, 1132 (1947).

tron-proton scattering experiments[4] at 12–13 Mev are in agreement with symmetrical tensor forces, but do not compare with the results obtained for a tensor force of the neutral or charged type.

Scattering experiments of 90-Mev neutrons by protons and deuterons were recently carried out in Berkeley.[5,6a] These data should enable one to still further eliminate phenomenological theories which are consistent with low energy scattering data. It should be mentioned here that the analysis of high energy scattering cross sections suffers from the serious drawback that, while relativistic effects may be important at energies as high as 100 Mev, the corresponding corrections of the non-relativistic calculations are yet unknown.[6b]

The present investigation pursues a twofold aim. Firstly, cross sections for high energy scattering are calculated for rectangular and Yukawa well shapes. The constants employed fit the binding energy of the deuteron, the epithermal *n-p* cross section, and the low energy *p-p* cross sections. This involves the assumption that *p-p* and *n-p* forces are essentially the same. It is investigated how the results change when different constants are assumed.[7] The first part deals with central forces, the second part with tensor forces. Actually, only tensor forces have significance, since it is not possible to account for the electric quadrupole moment of the deuteron under the assumption of central forces. Numerical results are obtained for various energies, including 100 Mev, and are compared with the Berkeley experiments.

Secondly, the phase method is applied to *n-p* and *n-n* scattering with tensor forces and—as in the case of central forces—the cross sections are given in terms of *real* phase shifts. The first calculations of scattering cross sections for tensor forces[8] and all those published since[9,10] yielded complex phase shifts, because the asymptotic form postulated for the eigenfunctions did not correspond to the partial waves which are characterized by constants of motion. The formulation in terms of real phase shifts appears to be more satisfactory from a theoretical point of view. Together with real phase shifts, it is necessary to introduce the amounts of admixture which measure the coupling between two states of different orbital angular momentum, but same total angular momentum and same parity. This coupling is due to the non-central character of tensor forces, and is introduced in a natural way by a unitary transformation from the LSM_LM_S scheme, in which the central force Hamiltonian is diagonal, to the $(-1)^LSJM$ scheme, in which the tensor force Hamiltonian is diagonal.

The phase shifts and the amounts of admixture are found by a variational procedure, since it is not possible to solve the occurring simultaneous differential equations in a closed form. The variational principle for the phase shifts was first given by Schwinger in his course on nuclear physics[11] where it was applied to S and D wave scattering.

We published some of our numerical results previously.[12] Meanwhile, a number of papers have appeared which deal with scattering by central[13,14] or tensor forces,[15,10] some of which overlap partly with our own calculations. This enables us to shorten certain parts of this report.[16] In particular, we refer to Ashkin and Wu[10] for the derivation of the scattering cross-section formulas for tensor forces in Born approximation.

The first part deals with central forces. The exact results which are obtained from the phase method (Section IA), are compared with the Born approximation (Section IB). The second

[4] J. S. Laughlin and P. G. Kruger, Phys. Rev. **73**, 197 (1948).

[5] Cook, McMillan, Peterson, and Sewell, Phys. Rev. **72**, 1264 (1948)L.

[6a] Hadley, Kelly, Leith, Segrè, Wiegand, and York, Phys. Rev. **73**, 1114 (1948)L.

[6b] For an estimate see: H. Snyder and R. E. Marshak, Phys. Rev. **72**, 1253 (1947).

[7] This is important, because recent experiments on the scattering of slow neutrons by ortho- and parahydrogen (R. B. Sutton *et al.* Phys. Rev. **72**, 1147 (1947)) and by hydrogen in crystals (C. G. Shull *et al.* Phys. Rev. **73**, 842 (1948)) indicate that the ranges of singlet and triplet forces may be much shorter than was commonly accepted, and may also be unequal to each other. See also: J. M. Blatt, Phys. Rev. **74**, 92 (1948).

[8] W. Rarita and J. Schwinger, Phys. Rev. **59**, 436 and 556 (1941).

[9] J. Jauch, Phys. Rev. **67**, 125 (1945).

[10] J. Ashkin and T. Y. Wu, Phys. Rev. **73**, 972 (1948).

[11] See also: J. Schwinger, Phys. Rev. **72**, 742 (1947)A.

[12] J. Eisenstein and F. Rohrlich, Phys. Rev. **73**, 641 and 1411 (1948).

[13] M. Camac and H. A. Bethe, Phys. Rev. **73**, 191 (1948).

[14] T. Y. Wu, Phys. Rev. **73**, 934, and 1132L (1948).

[15] H. S. W. Massey, E. H. S. Burhop, and T. M. Hu, Phys. Rev. **73**, 1403 (1948)L.

[16] For full details we refer to our theses (see the first note of this paper).

TABLE I. Total cross sections for neutron-proton scattering at 100 Mev. Central forces, exact calculations. (All values are in barns, i.e., 10^{-24} cm².)

Theory	$\sigma_{np}^{(s)}$	$\sigma_{np}^{(t)}$	σ_{np}
Neutral	0.0645	0.1939	0.1616
Charged	0.0552	0.1582	0.1325
Symmetric	0.1692	0.0921	0.1114*

* The value 0.094 obtained by Ta-You Wu (see reference 14, Table III) is due to a numerical error.

TABLE II. Total cross sections for neutron-neutron scattering at 100 Mev. Central forces, exact calculations. (All values are in barns, i.e., 10^{-24} cm².)

Theory	$\sigma_{nn}^{(s)}$	$\sigma_{nn}^{(t)}$	σ_{nn}
Neutral	0.0464	0.2289	0.1832
Charged	0.0464	0.1575	0.1297
Symmetric	0.0464	0.0252	0.0305

part is devoted to tensor forces. The results in Born approximation (Section IIA) are discussed, and the formulas for the differential and total cross section of *n-p* and *n-n* scattering are derived with the phase method (Section IIB). Numerical results are obtained by the aid of the variational principle for real phase shifts (Section IIC), and the comparison with the experiments is summarized. A list of formulas for *n-p* and *n-n* cross sections according to different theories is given in the appendix.

I. CENTRAL FORCES

A. The Phase Method

The assumption of central forces permits the direct application of the method of partial waves[17,18] or phase method. For each of the two spin states the space dependent part of the wave function can be written as the sum of the wave functions of fixed orbital angular momentum L. These functions are the solutions of a Schrödinger equation which, after separation of variables

$$\psi_L = \frac{u_L(r)}{r} P_L(\cos\theta) \tag{1}$$

lead to the radial equations

$$\left(\frac{d^2}{dr^2}+k^2-\frac{M}{\hbar^2}V(r)-\frac{L(L+1)}{r^2}\right)u_L(r)=0 \quad (L=0,\,1,\,2\cdots), \tag{2}$$

where

$$k^2=ME/\hbar^2. \tag{3}$$

M is the mass of the nucleon, E is the total energy in the center of mass system, and $V(r)$ is the potential energy. With a rectangular potential well of depth V_0 and range r_0 we can introduce the dimensionless quantities

$$x=r/r_0,\quad \kappa^2=MEr_0^2/\hbar^2=(kr_0)^2,\quad \lambda=MV_0r_0^2/\hbar^2 \tag{4}$$

and find for the wave function interior and exterior of the well,

$$\left(\frac{d^2}{dx^2}+\kappa^2\pm\lambda-\frac{L(L+1)}{x^2}\right)u_L^{(i)}(x)=0\quad (x<1), \tag{5}$$

$$\left(\frac{d^2}{dx^2}+\kappa^2-\frac{L(L+1)}{x^2}\right)u_L^{(e)}(x)=0\quad (x>1). \tag{6}$$

The $\pm$ sign corresponds to attractive and repulsive potential, respectively. The boundary conditions

$$u_L^{(i)}(0)=0,\quad u_L^{(e)}(\infty)\sim\sin\left(\kappa x+\frac{\pi L}{2}+\delta_L\right) \tag{7}$$

are fulfilled by the solutions

$$u_L^{(i)}(x)=xj_L(\kappa_1 x), \tag{8}$$

$$u_L^{(e)}(x)=Ax[j_L(\kappa x)-\tan\delta_L n_L(\kappa x)], \tag{9}$$

where

$$\kappa_1=(\kappa^2\pm\lambda)^{\frac{1}{2}}, \tag{10}$$

and

$$j_L(\kappa x)=\left(\frac{\pi}{2\kappa x}\right)^{\frac{1}{2}}J_{L+\frac{1}{2}}(\kappa x)\sim\frac{\sin(\kappa x-\pi L/2)}{\kappa x},$$
$$n_L(\kappa x)=\left(\frac{\pi}{2\kappa x}\right)^{\frac{1}{2}}N_{L+\frac{1}{2}}(\kappa x)\sim-\frac{\cos(\kappa x-\pi L/2)}{\kappa x} \tag{11}$$

are the spherical Bessel and Neumann functions,[19] respectively. Smoothness of the wave functions at the edge of the well requires the

[17] H. Faxen and J. Holtsmark, Zeits. f. Physik. **45**, 307 (1927).

[18] N. F. Mott and H. S. W. Massey, *Theory of Atomic Collisions* (The Clarendon Press, Oxford, 1935).

[19] See for example: J. Stratton, *Electromagnetic Theory* (McGraw-Hill Book Company, Inc., New York, 1941).

equality of the logarithmic derivatives

$$\left[\frac{d}{dx}\log u_L^{(i)}(x)\right]_{x=1}=\left[\frac{d}{dx}\log u_L^{(e)}(x)\right]_{x=1}. \quad (12)$$

Introducing (8) and (9) into (12), we find easily

$$\tan\delta_L=(-1)^L\frac{j_{L-1}(\kappa)-\dfrac{\kappa_1}{\kappa}\dfrac{j_{L-1}(\kappa_1)}{j_L(\kappa_1)}j_L(\kappa)}{j_{-L}(\kappa)+\dfrac{\kappa_1}{\kappa}\dfrac{j_{L-1}(\kappa_1)}{j_L(\kappa_1)}j_{-L-1}(\kappa)}, \quad (13)$$

where we made use of the identity

$$n_L(x)=(-1)^{L+1}j_{-L-1}(x).$$

The phase shifts can be evaluated from (13) by means of the tables[20] for j_L and j_{-L}. For strongly repulsive potentials as occur in the exchange theories, κ_1 of Eq. (10) may become imaginary. In this case (13) has to be replaced by

$$\tan\delta_L=(-1)^L\frac{j_{L-1}(\kappa)-\dfrac{|\kappa_1|}{\kappa}\dfrac{I_{L-\frac{1}{2}}(|\kappa_1|)}{I_{L+\frac{1}{2}}(|\kappa_1|)}j_L(\kappa)}{j_{-L}(\kappa)+\dfrac{|\kappa_1|}{\kappa}\dfrac{I_{L-\frac{1}{2}}(|\kappa_1|)}{I_{L+\frac{1}{2}}(|\kappa_1|)}j_{-L-1}(\kappa)}, \quad (14)$$

where[21]

$$I_L(\kappa)=i^{-L}J_L(ix).$$

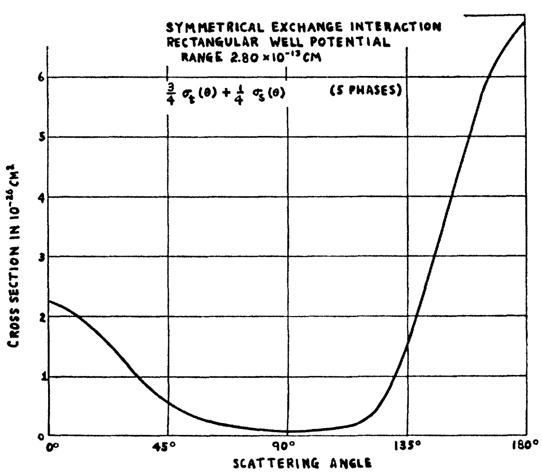

FIG. 1. Differential scattering cross section at 100 Mev.

[20] National Bureau of Standards, Mathematical Tables Project, *Tables of Spherical Bessel Functions*, Vol. I and II (Columbia University Press, New York, 1947).

[21] G. N. Watson, *Theory of Bessel Functions* (The Macmillan Company, New York, 1944).

The Eqs. (13) and (14) seem to us somewhat more convenient to use than the corresponding Eqs. (12) and (13) of Camac and Bethe.[13]

For the given well depths V_0 and for the even singlet and triplet states, we obtain from (4) two values, λ_s and λ_t, respectively. The value of κ_1 in (10) will in general depend on the parity $(-1)^L$ of the state and on the spin,

$$\kappa_1^{(s)}=(\kappa^2+\lambda_L^{(s)})^{\frac{1}{2}},\quad \kappa_1^{(t)}=(\kappa^2+\lambda_L^{(t)})^{\frac{1}{2}}. \quad (15)$$

For the neutral theory[8]

$$\lambda_L^{(s)}=\lambda_s,\quad \lambda_L^{(t)}=\lambda_t, \quad (16)$$

for the charged theory

$$\lambda_L^{(s)}=(-1)^L\lambda_s,\quad \lambda_L^{(t)}=(-1)^L\lambda_t, \quad (17)$$

and for the symmetrical theory

$$\lambda_L^{(s)}=-(1-2(-1)^L)\lambda_s,$$
$$\lambda_L^{(t)}=\tfrac{1}{3}(1+2(-1)^L)\lambda_t. \quad (18)$$

The phase shifts for these theories can now be calculated from (13) and (14). The differential cross section for n-p scattering is given by the well-known formula[17,18]

$$\sigma_{np}(\vartheta)=\left|\frac{1}{k}\sum_{L=0}^{\infty}(2L+1)e^{i\delta_L}\sin\delta_L P_L(\cos\vartheta)\right|^2, \quad (19)$$

and the total cross section by

$$\sigma_{np}=2\pi\int_0^{\pi}\sigma_{np}(\vartheta)\sin\vartheta d\vartheta$$
$$=\frac{4\pi}{k^2}\sum_{L=0}^{\infty}(2L+1)\sin^2\delta_L. \quad (20)$$

From these equations the n-n cross sections are obtained by the aid of the exclusion principle

$$\sigma_{nn}^{(s)}(\vartheta)=\left|\sum_{L=0}^{\infty}\frac{1+(-1)^L}{k}(2L+1)\times\exp(i\delta_L^{(s)})\sin\delta_L^{(s)}P_L(\cos\vartheta)\right|^2 \quad (21)$$

$$\sigma_{nn}^{(t)}(\vartheta)=\left|\sum_{L=0}^{\infty}\frac{1-(-1)^L}{k}(2L+1)\times\exp(i\delta_L^{(t)})\sin\delta_L^{(t)}P_L(\cos\vartheta)\right|^2, \quad (21)$$

and

$$\sigma_{nn} = \tfrac{1}{2} \cdot 2\pi \int_0^{\pi} \sigma_{nn}(\vartheta) \sin\vartheta d\vartheta \qquad (22)$$

since only half the number of deviated neutrons are scattered neutrons, the other half being recoil neutrons. When the two spin states are taken into account, one finds from (19) or (21) the two angular distributions $\sigma^{(s)}(\vartheta)$ and $\sigma^{(t)}(\vartheta)$. They combine in their respective weight 1:3 to give the total cross section

$$\sigma(\vartheta) = \tfrac{1}{4}\sigma^{(s)}(\vartheta) + \tfrac{3}{4}\sigma^{(t)}(\vartheta), \quad \sigma = \tfrac{1}{4}\sigma^{(s)} + \tfrac{3}{4}\sigma^{(t)}, \qquad (23)$$

with $\sigma^{(s)}$ and $\sigma^{(t)}$ from (20) or (22).

We adopted the ranges and well depths $r_s = 2.80 \times 10^{-13}$ cm, $V_0^s = 11.904$ Mev, and $r_t = 2.80 \times 10^{-13}$ cm, $V_0^t = 21.213$ Mev. For neutrons of 100-Mev energy in the laboratory system we find the total scattering cross sections as tabulated in Table I for *n-p* collisions and in Table II for *n-n* collisions. The angular distribution for *n-p* scattering in the symmetrical theory is plotted in Fig. 1. Its triplet part can be seen from Fig. 3.

It can be seen from Tables I and II that the magnitude of the potential influences the cross section much more than does its sign. In Table II only odd phases enter the triplet cross sections.

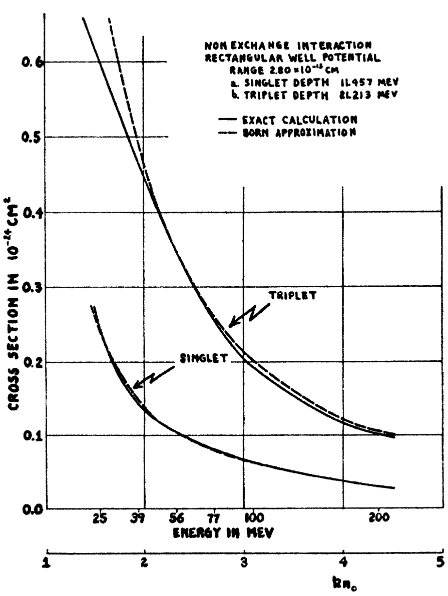

FIG. 2. Variation of singlet and triplet cross sections with energy.

TABLE IIIa. Variation of triplet *n-p* cross section with range at 25 Mev (central forces, exact calculations).

r_t (10^{-13} cm)	Neutral	Charged (barns)	Symmetric
1.8	0.4250	0.4130	0.4111
2.3	0.4657	0.4014	0.3931
2.8	0.6042	0.3891	0.3656

TABLE IIIb. Variation of triplet *n-p* cross section with range at 100 Mev (central forces, exact calculations).

r_t (10^{-13} cm)	Neutral	Charged (barns)	Symmetric
1.8	0.1351	0.0749	0.0613
2.8	0.1939	0.1582	0.0921

In the neutral and charged theory the magnitude of the potential is the same, but the odd states of the latter are repulsive rather than attractive. This causes a decrease of $\sigma_{nn}^{(t)}$ by one third, approximately. On the other hand, the charged and the symmetric theory have both repulsive odd states, but the magnitude of the potential in the latter is by two thirds smaller. This causes a decrease of $\sigma_{nn}^{(t)}$ by more than 80 percent. Qualitatively, the same behavior can be seen from $\sigma_{np}^{(t)}$ in Table I. In this case, however, it is less pronounced, because of the presence of even states which contribute equally in all three theories. As expected, the charged theory gives a somewhat smaller singlet cross section, $\sigma_{np}^{(s)}$, than does the neutral theory. The strong increase in $\sigma_{np}^{(s)}$ as we pass from the neutral to the symmetrical theory is due to the competition between a factor three and a minus sign. The repulsive P-state contributes 85 percent of the singlet *n-p* cross section in the symmetrical theory.

The total singlet and triplet *n-p* cross sections were calculated in the neutral theory for various energies between 25 and 200 Mev. They are plotted[22] in Fig. 2 and are in agreement with the results of Camac and Bethe.[13]

When we decrease the triplet range the triplet depth has to be increased correspondingly in order to account for the binding energy of the deuteron. We used Wiedenbeck and Marhoefer's

[22] It should be noted here that the singlet cross sections given in Fig. 2 were calculated with a potential well of 11.457 Mev rather than 11.904 Mev. The difference is practically negligible.

TABLE IV. Total cross sections for neutron-proton scattering at 100 Mev for central forces in Born approximation (rectangular well). All values are in barns (10^{-24} cm^2).

Theory	$\sigma_{np}^{(s)}$	$\sigma_{np}^{(t)}$	σ_{np}
Neutral and charged	0.0641	0.2034	0.1686
Symmetric	0.3872	0.0894	0.1639*

* The value 0.140 obtained by Ta-You Wu (see reference 14, Table III) is due to a numerical error (private communication of Dr. Wu).

TABLE V. Variation of triplet *n-p* cross section with range for central forces in Born approximation (rectangular well). All values are in barns.

Energy r_t	25 Mev. neutral and charged	100 Mev neutral and charged	Symmetric
1.8×10^{-13} cm	0.3578	0.1351	0.1121
2.3×10^{-13} cm	0.5522		0.0945
2.8×10^{-13} cm	0.7449	0.2034	0.0894

value[23] of 2.185 Mev. The well depths for three different triplet ranges are as follows:

$$\begin{array}{ll} r_t & V_0^{(t)} \\ 1.80\times10^{-13}\text{ cm} & 43.476\text{ Mev} \\ 2.30\times10^{-13}\text{ cm} & 28.963\text{ Mev} \\ 2.80\times10^{-13}\text{ cm} & 21.213\text{ Mev.} \end{array} \tag{24}$$

The variation of the triplet cross section with range is shown in Table IIIa for 25 Mev and in Table IIIb for 100 Mev.

Tables IIIa and IIIb show that the neutral theory leads to a smaller cross section when the range is reduced, independent of the energy. The charged and the symmetrical theory also give smaller cross sections for a reduced range, but only at higher energies (e.g., 100 Mev); at lower energies (e.g., 25 Mev) they lead to larger values. These results are in agreement with those obtained by Camac and Bethe (Table III).[13] The combined singlet and triplet cross section is seen from their table to increase with decreasing range ($r_s=r_t$) for energies below ~50 Mev for the charged theory and below ~60 Mev for the symmetrical theory.[24]

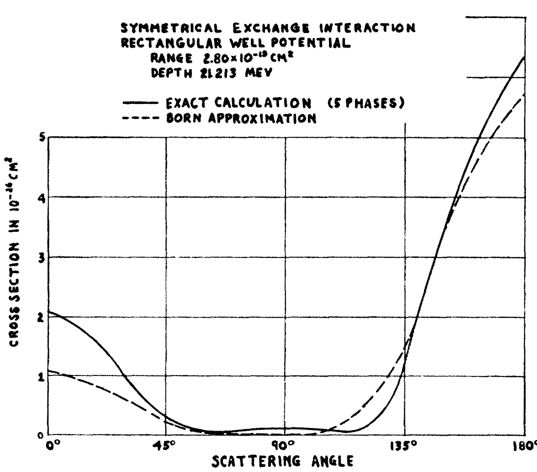

FIG. 3. Triplet differential cross section at 100 Mev.

Equation (15) shows that the decrease of the cross section due to the presence of exchange forces (charged or symmetric type) is relatively smaller the higher the energy. This effect can be so large that the cross section may even increase with energy. For example, the triplet *n-p* cross section in the charged theory is 0.155 barn at 80 Mev ($r_t=2.80\times10^{-13}$ cm), as calculated from the phase shifts of Camac and Bethe,[13] but is 0.158 barn at 100 Mev (Table I). On the other hand, the symmetrical theory increases the contribution to the singlet cross section of the odd states. Where an increase in energy leads to a strong increase in the contribution from an odd state, this may again lead to an increase of the cross section with energy. Thus we find $\sigma_{np}^{(s)}=0.164$ barn at 80 Mev (Camac and Bethe's phase shifts) and $\sigma_{np}^{(s)}=0.169$ barn at 100 Mev (Table I).

B. The Born Approximation

The formulas for the Born approximation are well known and need not be derived here. They are summarized in the Appendix.

Total cross sections for *n-p* scattering were calculated for a rectangular well with the constants given in IA. The results are shown in Fig. 2 for the neutral theory. The singlet cross section above ~25 Mev and the triplet cross section above ~40 Mev agree well with the exact calculations. At these neutron energies the total

[23] M. Wiedenbeck and C. Marhoefer, Phys. Rev. 67, 54 (1945)L.

[24] For 80 Mev Ta-You Wu obtained an apparent increase in the cross section with decreasing range in the symmetrical theory. (Phys. Rev. **73**, 1132 (1948)L, Table I.) His values 0.84 and 1.17×10^{-25} cm^2, however, should be interchanged. For the Gaussian potential the increase from 0.95 to 1.08×10^{-25} cm^2 is very probably only apparent, and is due to the use of the Born approximation (see Part I B, Table V).

TABLE VI. Total cross sections for *n-p* scattering at 100 Mev for central forces (Yukawa well, Born approximation). All values are in barns.

Theory	$\sigma_{np}^{(s)}$	$\sigma_{np}^{(t)}$	σ_{np}
Neutral or charged	0.0604	0.1309	0.1133
Symmetric	0.1545	0.0932	0.1086

energy in the center of mass system becomes comparable with the respective well depths, and the Born approximation ceases to hold. The curves for the Born approximation do not approach the curves for the exact calculations in a monotonic fashion, but oscillate and even cross the exact curves in the singlet case. This peculiar behavior is due to the sharp cut-off of the rectangular well.

In the Born approximation the total cross section in the charged theory is the same as in the neutral theory. At high energies (above $\sim$40 Mev) the charged theory leads actually to much smaller values than does the neutral theory. The situation is even worse for the symmetrical theory. For a range of 2.80×10^{-13} cm the triplet cross section is still in fair agreement with the exact value, but the singlet cross section is too large by a factor of two, even at 100 Mev. These relations are evident from a comparison between Table IV and Table I.

It follows from these remarks that the Born approximation is in general not reliable at 100 Mev. One obtains reasonably good approximate values, however, if one uses the combination

$$\sigma=\tfrac{1}{4}\sigma^{(s)}(\text{exact})+\tfrac{3}{4}\sigma^{(t)}(\text{Born}) \qquad (25)$$

for the symmetrical theory. If we decrease the triplet range, the well depth increases (see (24)), and for $r_t=1.8\times10^{-13}$ cm becomes nearly equal to the total energy in the center of mass system at 100-Mev neutron energy. The Born approximation will, therefore, not give good values. This is exhibited in Table V from which we drew first the erroneous conclusion that the cross section increases with decreasing range in the symmetrical theory at 100 Mev[12]. (See also reference 24.) On the other hand, the oscillatory character of the curves for the Born approximation (Fig. 2) may lead to relatively good agreement for energies as low as 25 Mev, as can be seen from a comparison of Table V with Table IIIa.

TABLE VII. Variation of triplet *n-p* cross section with range for central forces in Born approximation (Yukawa well) (energy: 100 Mev).

r_t 10^{-13} cm	$V_0^{(t)}$ Mev	Neutral or charged (barns)	Symmetric (barns)
1.089	78.070	0.110	0.0896
1.183	67.450	0.131	0.0932
2.177	24.203	0.191	0.1285
4.355	8.339	0.374	0.2241

Although the total triplet cross section at 100 Mev, symmetrical theory, is in Born approximation not very far off the exact value, the triplet differential cross section may lead to entirely erroneous quantitative conclusions. A fair qualitative agreement can be seen from Fig. 3. We find a ratio of backward to sideward scattering $R^{(t)}(\text{Born})=\sigma^{(t)}(\pi)/\sigma^{(t)}(\pi/2)=900$, whereas the exact value is $R^{(t)}(\text{exact})=78$.

It is of interest to examine how the assumption of different well shapes influences the cross section. A Yukawa potential of the type

$$V=V_0(e^{-x}/x), \quad (x=r/r_y), \qquad (26)$$

was, therefore, assumed, where r_Y is the "range" of the Yukawa potential. An analysis of proton-proton scattering[25] leads to a singlet range of $0.42\ e^2/mc^2=1.183\times10^{-13}$ cm, and to a singlet depth $V_0^{(s)}=89.65\ mc^2=45.80$ Mev. The triplet depths for various ranges follow from the binding energy of the deuteron by the use of a variational procedure.[26] They are listed in Table VII. If one assumes the triplet and singlet ranges to be equal, and chooses the above value of 1.183×10^{-13} cm, one finds in Born approximation the cross sections of Table VI.

For this Yukawa well the reduction of the neutral cross section due to symmetrical exchange forces is much smaller than for a rectangular well of ranges 2.80×10^{-13} cm. The Born approximation for the neutral theory will not be far off the exact value. From calculations by Chew and Goldberger[27] we may conclude that

[25] L. E. Hoisington, S. S. Share, and G. Breit, Phys. Rev. **56**, 884 (1939).

[26] L. Hulthen, Arkiv. f. Mat., Astr. o. Fys. **28A**, No. 5 (1942).

[27] G. F. Chew and M. L. Goldberger, Phys. Rev. **73**, 1409 (1948)L. For 80 Mev the Born approximation for a Yukawa well gives 0.131 barn; their value of 0.150 barn is due to an error (private communication).

TABLE VIII. Total n-p cross sections for a rectangular well at 100 Mev (tensor forces, Born approximation). All values in barns.

Theory	$\sigma_{\mathrm{Born}}^{(t)}$	σ_{Born}	$\frac{1}{4}\sigma_{ex}^{(s)}+\frac{3}{4}\sigma_{\mathrm{Born}}^{(t)}$	$R=\frac{\sigma(\pi)}{\sigma(\pi/2)}$
Neutral or charged	0.2516	0.2047	0.2048	0.30 or 3.75
Symmetric	0.0939	0.1672	0.1127	7.9

TABLE IX. Variation of triplet n-p cross section with range for 100 Mev (tensor forces, Born approximation, rectangular well).

r_t 10^{-13} cm	γ	V_0 Mev	Q 10^{-27} cm^2	D-state percent	Neutral barns	Symmetric barns
2.80	0.775	13.89	2.73	3.9	0.2516	0.0939
2.30	1.564	15.92	2.73	6.9	0.4216	
2.30	1.292	13.55	2.16	4.0	0.1835	0.102

the cross section in the symmetrical theory is at 100 Mev smaller than the exact value by about 6 percent or less. It follows that this well leads to considerably smaller neutral cross sections than the rectangular well ($r_s=r_t=2.80\times10^{-13}$ cm) at 100 Mev, and to about equal or somewhat larger values for the symmetrical theory. At 80 Mev the symmetrical theory leads to much larger cross sections with a Yukawa well,[27] 0.140 barns instead of 0.111 barn.

As in the case of a rectangular well a range reduction causes a decrease of the cross section. Since the error made in the Born approximation for the symmetrical theory is much smaller for a Yukawa well than it is for a rectangular well, we can be sure that the qualitative behavior exhibited by the Born approximation is correct; the various triplet cross sections are given in Table VII.

II. TENSOR FORCES

A. The Born Approximation

The inclusion of tensor forces in the nucleon interaction effects only the triplet states, since the tensor operator

$$S_{12}=3(\sigma_1\cdot r,\ \sigma_2\cdot r/r^2)-\sigma_1\cdot\sigma_2 \qquad (27)$$

vanishes for singlet states. The triplet potential is

$$V(r)=f(\sigma_1\cdot\sigma_2,\ \tau_1\cdot\tau_2)[J(r)+\gamma S_{12}K(r)], \qquad (28)$$

where γ is a constant and $f(\sigma_1\cdot\sigma_2,\ \tau_1\cdot\tau_2)$ is for the neutral theory

$$f=-1, \qquad (29)$$

for the charged theory

$$f=(1+\sigma_1\cdot\sigma_2/2)(1+\tau_1\cdot\tau_2/2), \qquad (30)$$

and for the symmetrical theory

$$f=\tfrac{1}{3}\sigma_1\cdot\sigma_2,\ \tau_1\cdot\tau_2. \qquad (31)$$

Let

$$R=(-1)^L,\quad S=\frac{1+\sigma_1\cdot\sigma_2}{2},\quad T=\frac{1+\tau_1\cdot\tau_2}{2} \qquad (32)$$

be the space, spin, and isotopic spin symmetry operator, respectively. Then the exclusion principle requires that the wave function be anti-

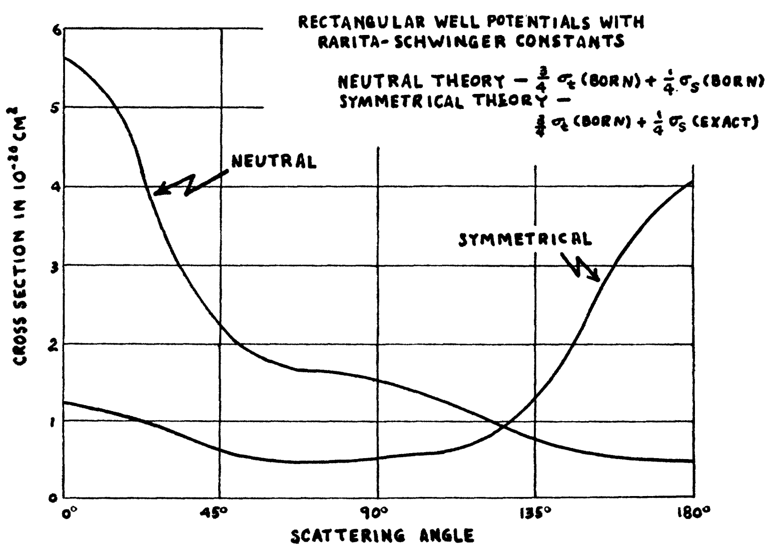

FIG. 4. Differential cross sections at 100 Mev for tensor force theories.

symmetric in the operator RST, i.e.,

$$\mathrm{RST} = -1. \tag{33}$$

If, furthermore, the particles are identical, i.e., they are two neutrons or two protons, $T=1$. These relations determine $f(\sigma_1\cdot\sigma_2,\ \tau_1\cdot\tau_2)$ uniquely and in agreement with Eqs. (16)–(18).

The constant γ can be so determined that

$$J(r)=V_0F(x),\quad K(r)=V_0G(x),\quad x=r/r_0. \tag{34}$$

With this potential the differential and total cross section can easily be derived in Born approximation.[10] The results are given in the appendix.

In what follows we will assume that the two shape factors $F(x)$ and $G(x)$ are equal. For this case and a rectangular well shape

$$F(x)=1\quad (x<1),\qquad F(x)=0\quad (x>1),$$

the constants were determined by Rarita and Schwinger:[8] $r_0=2.80\times10^{-13}$ cm, $V_0=13.89$ Mev, $\gamma=0.775$. The triplet cross sections obtained with these constants are shown in Table VIII. The singlet cross sections are, of course, the same as without tensor forces, and are known exactly (Table I) and in Born approximation (Table IV). It is, therefore, easy to obtain the combination (25) for the total cross section which is much closer to the exact solution, especially for the symmetrical theory. This is also given in Table VIII.

The results in column 2 of Table VIII are in agreement with those of Ashkin and Wu.[10] The differential cross section in Born approximation was also given by these authors. Since the combination (25), however, gives much better results than the actual Born approximation, we have plotted the angular distribution for this combination (Fig. 4). We observe an appreciable increase of the scattering at right angles as a result of the tensor force. (Compare Figs. 1 and 4.) The backward scattering in the symmetrical theory decreased strongly. The total cross sections are larger for tensor forces than for central forces.

In order to examine the effect of a reduced triplet range we proceed as follows. Since it is not possible to fit both, the quadrupole moment of the deuteron and the amount of D-state, with other constants than those given by Rarita and Schwinger,[8] we evaluated two sets of constants, one that fits the quadrupole moment and another that fits the D-state. We assumed a reduced range of 2.3×10^{-13} cm and used a variational procedure to determine the constants. The results are given in the following Table IX. Since a reduced range makes the angular distribution more isotropic (less contributions from higher angular momenta), it is clear that more D-state is required to fit the same quadrupole moment. The constant γ increases very strongly with decreasing range. As was pointed out in our Letter,[12] this effectively decreases the ratio of backward to sideward scattering. The cross section, however, reduces strongly in the neutral theory only, and increases even there if we try to fit the quadrupole moment.

For a Yukawa tensor potential constants were calculated by Feshbach, Eisenstein, and

TABLE X. Constants for a Yukawa tensor potential.*

	r_t(central) 10^{-13} cm	Meson mass electron masses	r_t(tensor) 10^{-13} cm	Meson mass electron masses	$V_0^{(t)}$ Mev	γ
(I)	1.202	321	1.400	276	30.817	1.459
(II)	1.202	321	1.556	248	45.286	0.618

* See reference 28.

TABLE XI. Total n-p cross section for a Yukawa well and a symmetrical theory at 100 Mev (tensor forces, Born approximation). All values are in barns.

Constants	$\sigma^{(t)}$	σ	$R=\sigma(\pi)/\sigma(\pi/2)$
(I)	0.0674	0.0892	9.08
(II)	0.0760	0.0956	12.2

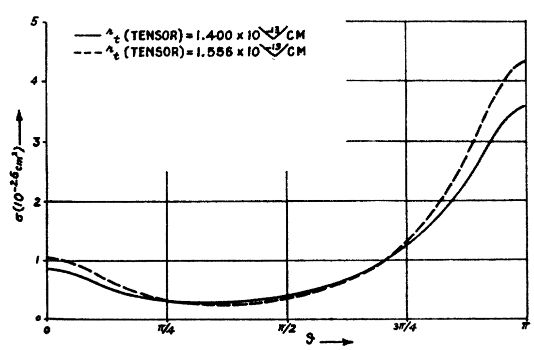

FIG. 5. Differential cross sections at 100 Mev for tensor forces and a Yukawa potential (symmetrical theory).

Schwinger.[28] They assumed a Yukawa well shape (26) for both shape functions (34), but different ranges, r_t(central) and r_t(tensor), for the central and tensor part of the triplet potential, respectively. They found two different sets of constants which fit the quadrupole moment of the deuteron (Table X). The singlet range and depth are the same as in the non-tensor case. Using the Born approximation one obtains from these constants the differential cross sections of Fig. 5 and the total cross sections as given in Table XI above. These total cross sections are smaller than those obtained for a rectangular tensor potential or for a Yukawa non-tensor potential. The ratios R are about the same as for the rectangular tensor potential, but they cannot be trusted too much because of the Born approximation.

B. The Phase Method for Tensor Forces

In the case of central forces the spin and the orbital angular momentum are constants of motion. One uses, therefore, the representation which is characterized by the four quantum numbers LSM_LM_S. When tensor forces are present the magnitude and the z-component of the orbital angular momentum are no longer constants of motion; neither is the z-component of the spin angular momentum. Only the square of the spin angular momentum commutes with the tensor Hamiltonian. It follows that a transformation to the $LSJm$ scheme, where J and m characterize the magnitude and the z-component of the total angular momentum, will not diagonalize the tensor Hamiltonian. A further transformation to the $(-1)^LSJm$ scheme is required. The parity operator, whose eigenvalues are $(-1)^L$, commutes with the tensor Hamiltonian.

Again, the tensor force operator S_{12} enters only in triplet states. In the LSM_LM_S scheme the angular dependence is described by the spherical harmonics $Y_L^{M_L}(\vartheta, \varphi)$. A transformation to the $LSJM$ scheme yields

$$\phi_{L,J}{}^m(\vartheta, \varphi) = \sum_{M_L, M_S} Y_L{}^{M_L}(\vartheta, \varphi)\chi_S{}^{M_S} \times (LSM_LM_S/LSJm), \quad (35)$$

where $\chi_S{}^{M_S}$ is the spin wave function. For triplet states the function $\phi_{LJ}{}^m$ can be regarded as a vector, $\boldsymbol{\Phi}_{L,J'}{}^m$ in the three-dimensional orthonormal space spanned by the vectors

$$\frac{1}{\sqrt{2}}(\chi_1{}^1+\chi_1{}^{-1}), \quad \frac{i}{\sqrt{2}}(\chi_1{}^1-\chi_1{}^{-1}), \quad \chi_1{}^0.$$

The vector $\boldsymbol{\Phi}_{L,J}{}^m$ was discussed in detail by Corben and Schwinger[29] and by Rarita and Schwinger.[8]

In complete analogy to the case of central forces we separate the Schrödinger equation

$$\left[\nabla^2+\frac{M}{\hbar^2}(E-V)\right]\Psi=0, \quad (36)$$

into partial waves, according to the $LSJm$ scheme, first,

$$\Psi = \sum_{J,m} c_J{}^m\psi_J{}^m, \quad \psi_J{}^m = \sum_J c_L\psi_{L,J}{}^m \quad (L=J-1,\ J,\ J+1). \quad (37)$$

Separation of variables can now be achieved by putting

$$\psi_{J-1,J} = \frac{u_J(r)}{r}\boldsymbol{\Phi}_{J-1,J}, \quad \psi_{J,J}{}^m = \frac{v_J(r)}{r}\boldsymbol{\Phi}_{J,J}{}^m,$$
$$\overset{m}{\psi}_{J+1,J} = \frac{w_J(r)}{r}\overset{m}{\boldsymbol{\Phi}}_{J+1}. \quad (38)$$

The operator S_{12} will couple states of equal parity[8]

$$S_{12}\overset{m}{\boldsymbol{\Phi}}_{J-1,J} = -2\frac{J-1}{2J+1}\overset{m}{\boldsymbol{\Phi}}_{J-1,J} + 6\frac{[J(J+1)]^{\frac{1}{2}}}{2J+1}\overset{m}{\boldsymbol{\Phi}}_{J+1,J},$$
$$S_{12}\overset{m}{\boldsymbol{\Phi}}_{J+1,J} = 6\frac{[J(J+1)]^{\frac{1}{2}}}{2J+1}\overset{m}{\boldsymbol{\Phi}}_{J-1,J} - 2\frac{J+2}{2J+1}\overset{m}{\boldsymbol{\Phi}}_{J+1,J}, \quad (39)$$
$$S_{12}\boldsymbol{\Phi}_{J,J}{}^m = 2\boldsymbol{\Phi}_{J,J}{}^m.$$

When we introduce (37) and (38) into the Schrödinger equation (36) and observe (39), we

[28] H. Feshbach, J. Eisenstein, and J. S. Schwinger, Phys. Rev. **74**, 1223 (1948).

[29] H. C. Corben and J. S. Schwinger, Phys. Rev. **58**, 953 (1940).

obtain three radial equations for each value of J. The case $J=0$ is a trivial exception. With the potential (28) we find with the dimensionless quantities (4) and (34)

$$\begin{aligned}
&\left(\frac{d^2}{dx^2}+\kappa^2-\frac{J(J-1)}{x^2}\right)u_J(x)\\
&\qquad=f(\sigma_1\cdot\sigma_2,\ \tau_1\cdot\tau_2)\\
&\qquad\qquad\times\lambda(f_J(x)u_J(x)+g_J(x)w_J(x)),\\
&\left(\frac{d^2}{dx^2}+\kappa^2-\frac{(J+1)(J+2)}{x^2}\right)w_J(x)\\
&\qquad=f(\sigma_1\cdot\sigma_2,\ \tau_1\cdot\tau_2)\\
&\qquad\qquad\times\lambda(g_J(x)u_J(x)+h_J(x)w_J(x)),\\
&\left(\frac{d^2}{dx^2}+\kappa^2-\frac{J(J+1)}{x^2}\right)v_J(x)\\
&\qquad=f(\sigma_1\cdot\sigma_2,\ \tau_1\cdot\tau_2)\lambda l(x)v_J(x),
\end{aligned}\tag{40}$$

where

$$\begin{aligned}
f_J(x)&=F(x)-2\frac{J-1}{2J+1}\gamma G(x),\\
g_J(x)&=6\frac{[J(J+1)]^{\frac{1}{2}}}{2J+1}\gamma G(x),\\
h_J(x)&=F(x)-2\frac{J+2}{2J+1}\gamma G(x),\\
l(x)&=F(x)+2\gamma G(x).
\end{aligned}\tag{41}$$

The first two differential equations are coupled, the third one is uncoupled. They are equivalent to the three integral equations

$$\begin{aligned}
u_J(x)&=A_J\kappa xj_{J-1}(\kappa x)-f\lambda\int_0^\infty G_J{}^u(x,x')\\
&\qquad\times[f_J(x')u_J(x')+g_J(x')w_J(x')]dx',\\
w_J(x)&=C_J\kappa xj_{J+1}(\kappa x)-f\lambda\int_0^\infty G_J{}^w(x,x')\\
&\qquad\times[g_J(x')u_J(x')+h_J(x')w_J(x')]dx',\\
v_J(x)&=B_J\kappa xj_J(\kappa x)-f\lambda\int_0^\infty G_J{}^v(x,x')\\
&\qquad\times l(x')v_J(x')dx',
\end{aligned}\tag{42}$$

where

$$\begin{aligned}
G_J{}^u(x,x')&=-\frac{1}{\kappa}\cdot\kappa x_<j_{J-1}(\kappa x_<)\cdot\kappa x_>n_{J-1}(\kappa x_>),\\
G_J{}^w(x,x')&=-\frac{1}{\kappa}\cdot\quad j_{J+1}(\kappa x_<)\cdot\kappa x_>n_{J+1}(\kappa x_>),\\
G_J{}^v(x,x')&=-\frac{1}{\kappa}\cdot\kappa x_<j_J(\kappa x_<)\cdot\kappa x_>n_J(\kappa x_>).
\end{aligned}\tag{43}$$

are the appropriate symmetrical Green's functions. They satisfy the equations

$$\left(\frac{d}{dx^2}+\kappa^2-\frac{J(J-1)}{x^2}\right)G_J{}^u(x,x')=-\delta(x-x'),\quad\text{etc.}\tag{44}$$

and vanish at $x_<=0$. The notation $x_<$ and $x_>$ is convenient to designate respectively the smaller and the larger of x and x'.

It follows from the asymptotic relations (11) that for large x the Eqs. (42) become

$$\begin{aligned}
u_J(x)&\sim A_J\sin\left(\kappa x-(J-1)\frac{\pi}{2}\right)\\
&\quad-f\frac{\lambda}{\kappa}\cos\left(\kappa x-(J-1)\frac{\pi}{2}\right)\int_0^\infty\kappa x'j_{J-1}(\kappa x')\\
&\qquad\times(f_Ju_J+g_Jw_J)dx',\\
w_J(x)&\sim C_J\sin\left(\kappa x-(J+1)\frac{\pi}{2}\right)\\
&\quad-f\frac{\lambda}{\kappa}\cos\left(\kappa x-(J+1)\frac{\pi}{2}\right)\int_0^\infty\kappa x'j_{J+1}(\kappa x')\\
&\qquad\times(g_Ju_J+h_Jw_J)dx',\\
v_J(x)&\sim B_J\sin\left(\kappa x-\frac{J\pi}{2}\right)\\
&\quad-f\frac{\lambda}{\kappa}\cos\left(\kappa x-\frac{J\pi}{2}\right)\int_0^\infty\kappa x'j_J(\kappa x')l_Jv_Jdx'.
\end{aligned}\tag{45}$$

The asymptotic form required for our solutions may be written†

† In this form the phase shifts will in general also depend on m (see reference 30b).

$$u_J(x) \sim \frac{A_J}{\cos\delta_J{}^u} \sin\left(\kappa x - (J-1)\frac{\pi}{2} + \delta_J{}^u\right)$$
$$= A_J \sin\left(\kappa x - (J-1)\frac{\pi}{2}\right)$$
$$+ A_J \tan\delta_J{}^u \cos\left(\kappa x \quad (J-1)\frac{\pi}{2}\right), \quad (46)$$
$$w_J(x) \sim \frac{C_J}{\cos\delta_J{}^w} \sin\left(\kappa x - (J+1)\frac{\pi}{2} + \delta_J{}^w\right),$$
$$v_J(x) \sim \frac{B_J}{\cos\delta_J{}^v} \sin\left(\kappa x - \frac{J\pi}{2} + \delta_J{}^v\right).$$

A comparison of (45) and (46) yields to the determination of the constants

$$A_J = -\cot\delta_J{}^u \cdot f\lambda \int_0^\infty j_{J-1}(\kappa x')[f_J(x')u_J(x') + g_J(x')w_J(x')]x'dx',$$
$$C_J = -\cot\delta_J{}^w \cdot f\lambda \int_0^\infty j_{J+1}(\kappa x')[g_J(x')u_J(x') + l(x')w_J(x')]x'dx', \quad (47)$$
$$B_J = -\cot\delta_J{}^v \cdot f\lambda \int_0^\infty j_J(\kappa x')l(x')v_J(x')x'dx'.$$

With the aid of these equations we can express the formal solutions (42) in terms of the phase shifts

$$u_J(x) = -\cot\delta_J{}^u f\lambda \cdot \kappa x j_{J-1}(\kappa x) \times \int_0^\infty j_{J-1}(\kappa x')[f_J u_J + g_J w_J]x'dx' - f\lambda \int_0^\infty G_J{}^u(x, x')[f_J u_J + g_J w_J]dx',$$
$$w_J(x) = -\cot\delta_J{}^w f\lambda \cdot \kappa x j_{J+1}(\kappa x) \times \int_0^\infty j_{J+1}(\kappa x')[g_J u_J + h_J w_J]x'dx' - f\lambda \int_0^\infty G_J{}^w(x, x')[g_J u_J + h_J w_J]dx', \quad (48)$$
$$v_J(x) = -\cot\delta_J{}^v f\lambda \cdot \kappa x j_J(\kappa x) \times \int_0^\infty j_J(\kappa x')l v_J(x')x'dx' - f\lambda \int_0^\infty G_J{}^v(x, x')l v_J dx'.$$

Since L can take on the values $J-1$, J, and $J+1$, the wave functions in the $(-1)^L SJm$ scheme will either be the same as those in the $LSJm$ scheme, namely when $L=J$, or they will be linear combinations of $\psi_{J-1,J}{}^m$ and $\psi_{J+1,J}{}^m$, which have the same parity. In the latter case there will be two independent wave functions for each value of J. We denote them by $\psi_{J,m}{}^\alpha$ and $\psi_{J,m}{}^\gamma$, respectively.

$$\psi_{J,m}{}^\alpha = \frac{1}{x}u_J{}^\alpha(x)\overset{m}{\mathbf{\Phi}}_{J-1,J} - \frac{1}{x}w_J{}^\alpha(x)\overset{m}{\mathbf{\Phi}}_{J+1,J},$$
$$\psi_{J,m}{}^\gamma = \frac{1}{x}u_J{}^\gamma(x)\overset{m}{\mathbf{\Phi}}_{J-1,J} - \frac{1}{x}w_J{}^\gamma(x)\overset{m}{\mathbf{\Phi}}_{J+1,J}, \quad (49)$$
$$\psi_{J,m}{}^\beta = \frac{1}{x}v_J(x)\mathbf{\Phi}_{J,J}{}^m = \psi_{J,J}{}^m.$$

These are the three eigenfunctions of the tensor Hamiltonian in the $(-1)^L SJm$ representation. If we want to write the total wave function Ψ of (36) as the sum of partial waves which are all "eigenwaves," as in the case of central forces, we have to replace the second sum in (37) by

$$\psi_J{}^m = c_\alpha\psi_{J,m}{}^\alpha + c_\beta\psi_{J,m}{}^\beta + c_\gamma\psi_{J,m}{}^\gamma. \quad (37')$$

Each of these partial waves is, therefore, defined by J, m, and one of the three indices α, β, γ. The wave function ψ_{total} which is the sum of the wave functions for the incident and the scattered wave, will also be the sum of partial waves defined by these quantum numbers. For any one of these waves we now require that its radial part differ asymptotically from the radial part of the corresponding incoming partial wave only by a phase shift. In other words, the asymptotic forms (46) have to be chosen such that (49) becomes—apart from constant factors

$$\psi_{J,m}{}^\alpha \sim \frac{1}{x}\sin(\kappa x - (J-1)\pi/2 + \delta_J{}^\alpha) \times (\overset{m}{\mathbf{\Phi}}_{J-1,J} + \eta_J{}^\alpha \overset{m}{\mathbf{\Phi}}_{J+1,J}),$$
$$\psi_{J,m}{}^\gamma \sim \frac{1}{x}\sin(\kappa x - (J+1)\pi/2 + \delta_J{}^\gamma) \times (\overset{m}{\mathbf{\Phi}}_{J-1,J} + \eta_J{}^\gamma \overset{m}{\mathbf{\Phi}}_{J+1,J}), \quad (50)$$
$$\psi_{J,m}{}^\beta \sim \frac{1}{x}\sin(\kappa x - J\pi/2 + \delta_J{}^\beta)\mathbf{\Phi}_{J,J}{}^m.$$

The function $v_J(x)$ is, therefore, not effected ($\delta_J{}^\beta=\delta_J{}^v$). For $u_J(x)$ and $w_J(x)$, however, $\delta_J{}^u$ equals $\delta_J{}^w$ for each set α and γ, respectively.

$$u_J{}^{\alpha,\gamma}(x)\sim\sin(\kappa x-(J-1)\pi/2+\delta_J{}^{\alpha,\gamma}),$$
$$w_J{}^{\alpha,\gamma}(x)\sim\eta_J{}^{\alpha,\gamma}\sin(\kappa x-(J+1)\pi/2+\delta_J{}^{\alpha,\gamma}). \quad (46')$$

The eigenfunctions $\psi_{J,m}{}^\alpha$ and $\psi_{J,m}{}^\gamma$ of (49) are uniquely determined by this requirement of equal phase shifts for $u_J(x)$ and $w_J(x)$. It corresponds to a diagonalization of the scattering matrix which would otherwise be diagonal only for the states $L=J$, i.e., for the wave functions $\psi_{J,m}{}^\beta$. The phase shifts $\delta_J{}^\alpha$, $\delta_J{}^\beta$, and $\delta_J{}^\gamma$, which are defined by (46′) and (50) are all real.

The constants η_J follow from (46) and (46′) with $\delta_J{}^u=\delta_J{}^w$,

$$\eta_J=\text{asymptotic form of}\left(-\frac{w_J(x)}{u_J(x)}\right)=\frac{C_J}{A_J}, \quad (51)$$

and can easily be evaluated from (47) as will be shown in Section C. Since the orthogonality integrals of the wave functions (49) exist only in the limit

$$\lim_{x\to\infty}\left(\int_0^x u_\alpha(x)u_\gamma(x)dx\right)\Big/\left(\int_0^x u_\alpha{}^2(x)dx\right)^{\frac{1}{2}}\left(\int_0^x u_\gamma{}^2(x)dx\right)^{\frac{1}{2}},$$

only the asymptotic forms (50) will contribute, and one finds that the constants η_J satisfy the identity

$$\eta_J{}^\alpha\eta_J{}^\gamma=-1. \quad (52)$$

These constants are called the amounts of admixture. For definiteness we shall always denote the numerically smaller of them by $\eta_J{}^\alpha$. In the limit, as the tensor part of the potential goes to zero, $\eta_J{}^\alpha\rightarrow\pm 0$ and $\eta_J{}^\gamma\rightarrow\mp\infty$; the eigenfunctions, $\psi_{J,m}{}^\alpha$ and $\psi_{J,m}{}^\gamma$, become identical with $\psi_{J-1,J}{}^m$ and $\psi_{J+1,J}{}^m$, respectively, in this limit.†† It follows that $\eta_J{}^\alpha$ measures the amount of admixture of the state $L=J+1$ to the state $L=J-1$, and that $1/\eta_J{}^\gamma=-\eta_J{}^\alpha$ is the amount of admixture of the state $L=J-1$ to the state $L=J+1$.

We may now derive the formulas for the differential and total triplet cross section. For this purpose we transform the incident plane wave into the $LSJm$ representation which is the same as the $(-1)^LSJm$ scheme in the absence of a potential. In the LSM_LM_S representation

$$\psi_{\text{inc}}{}^{M_S}=\sum_L(2L+1)i^Lj_L(\kappa x)P_L(\cos(\widehat{\kappa\mathbf{x}}))\chi_1{}^{M_S}.$$

The inverse of the transformation (35) with the appropriate normalization factor gives

$$\psi_{\text{inc}}{}^m=(4\pi)^{\frac{1}{2}}\sum_L(2L+1)^{\frac{1}{2}}i^Lj_L(\kappa x)\times\sum_J\mathbf{\Phi}_{LJ}{}^m(L1Jm|L10m)$$
$$\sim\frac{(4\pi)^{\frac{1}{2}}}{\kappa x}\sum_J\sum_L(2L+1)^{\frac{1}{2}}i^L\times\sin\left(\kappa x-\frac{\pi L}{2}\right)\mathbf{\Phi}_{LJ}{}^m(L1Jm|L10m), \quad (53)$$

where we used again the vector notation $\mathbf{\Phi}_{L,J}{}^m$. Since $m=M_L+M_S$ is a constant of motion and $M_L=0$ for the plane wave, one has always $m=M_S{}^{\text{inc}}$. The transformation matrix $(L1JM|L10m)$ is given in Table XII.[30a]

The asymptotic form of the total wave, i.e., the incident wave and the scattered wave will contain the tensor force eigenfunctions (49) in their asymptotic form (50)

$$\overset{m}{\psi}_{\text{total}}\sim\frac{(4\pi)^{\frac{1}{2}}}{\kappa x}\sum_J\{\alpha_J{}^m\exp(i\delta_J{}^\alpha)[i^{J-1}\sin(\kappa x-(J-1)\pi/2+\delta_J{}^\alpha)\overset{m}{\mathbf{\Phi}}_{J-1,J}$$
$$+\eta_J{}^\alpha i^{J+1}\sin(\kappa x-(J+1)\pi/2+\delta_J{}^\alpha)\overset{m}{\mathbf{\Phi}}_{J+1,J}]+\beta_J{}^m\exp(i\delta_J{}^\beta)i^J\sin(\kappa x-J\pi/2+\delta_J{}^\beta)\mathbf{\Phi}_{J,J}{}^m$$
$$+\gamma_J{}^m\exp(i\delta_J{}^\gamma)[i^{J-1}\sin(\kappa x-(J-1)\pi/2+\delta_J{}^\gamma)\overset{m}{\mathbf{\Phi}}_{J-1,J}$$
$$+\eta_J{}^\gamma i^{J+1}\sin(\kappa x-(J+1)\pi/2+\delta_J{}^\gamma)\overset{m}{\mathbf{\Phi}}_{J+1,J}]. \quad (55)$$

†† Actually, $\eta_J{}^\alpha$ is always positive or zero.

[30a] E. U. Condon and G. H. Shortley, *Theory of Atomic Spectra* (The Macmillan Company, New York, 1935), p. 76. Note, however, that the table is written in terms of J rather than L, and that the phases are chosen different in order to comply with the choice of phases in the definitions of $\Phi_{LJ}{}^m$ (reference 29).

TABLE XII. $(2L+1)^{\frac{1}{2}}\,(L1Jm|L10m)$.

$L \backslash m$	± 1	0	
$J-1$	$\mp((J-1)/2)^{\frac{1}{2}}$	$J^{\frac{1}{2}}$	
J	$((2J+1)/2)^{\frac{1}{2}}$	0	(54)
$J+1$	$\pm(J/2)^{\frac{1}{2}}$	$(J+1)^{\frac{1}{2}}$	

The constants,[30b] $\alpha_J{}^m$, $\beta_J{}^m$, and $\gamma_J{}^m$ are found by comparing this expression for vanishing potential ($\delta_J{}^\alpha=\delta_J{}^\beta=\delta_J{}^\gamma=0$) with the plane wave (53)

$$\alpha_J{}^{\pm1}=\mp\frac{(J+1)^{\frac{1}{2}}-\eta_J{}^\alpha J^{\frac{1}{2}}}{\sqrt{2}[1+(\eta_J{}^\alpha)^2]},\quad \alpha_J{}^0=\frac{J^{\frac{1}{2}}+\eta_J{}^\alpha(J+1)^{\frac{1}{2}}}{1+(\eta_J{}^\alpha)^2},$$

$$\beta_J{}^m=|m|\left(\frac{2J+1}{2}\right)^{\frac{1}{2}},\tag{56}$$

$$\gamma_J{}^{\pm1}=\mp\frac{(J+1)^{\frac{1}{2}}-\eta_J{}^\gamma J^{\frac{1}{2}}}{\sqrt{2}[1+(\eta_J{}^\gamma)^2]},\quad \gamma_J{}^0=\frac{J^{\frac{1}{2}}+\eta_J{}^\gamma(J+1)^{\frac{1}{2}}}{1+(\eta_J{}^\gamma)^2}.$$

The factors $e^{i\delta_J}$ in (55) have been chosen such that the scattered wave is a purely outgoing wave. It is found by subtracting the incident wave (53) from the total wave (55),

$$\overset{m}{\psi}_{\text{scatt}}\sim\frac{e^{ikr}}{r}\frac{(4\pi)^{\frac{1}{2}}}{k}\sum_J[\alpha_J{}^m\exp(i\delta_J{}^\alpha)\times\sin\delta_J{}^\alpha(\overset{m}{\mathbf{\Phi}}_{J-1,J}+\eta_J{}^\alpha\overset{m}{\mathbf{\Phi}}_{J+1,J})+\beta_J{}^m\exp(i\delta_J{}^\beta)\sin\delta_J{}^\beta\mathbf{\Phi}_{J,J}{}^m+\gamma_J{}^m\exp(i\delta_J{}^\gamma)\sin\delta_J{}^\gamma\times(\overset{m}{\mathbf{\Phi}}_{J-1,J}+\eta_J{}^\gamma\overset{m}{\mathbf{\Phi}}_{J+1,J})].\tag{57}$$

The differential cross section for polarized beams of neutrons and protons (fixed m) is the square of the absolute value of the coefficient of e^{ikr}/r of the scattered wave (57)

$$\sigma_t{}^m(\vartheta)=4\pi/k^2|\textstyle\sum_J[\cdots]|^2.\tag{58}$$

If the incident neutrons are unpolarized we have to average over m

$$\sigma_t(\vartheta)=(4\pi/3k^2)\textstyle\sum_m|\sum_J[\cdots]|^2.\tag{59}$$

The total cross section is found by integration over all the angles. The cross terms vanish, because of the orthogonality of the $\Phi_{L,J}{}^m$ and because of (52), and one finds with (56) after summation over m for the triplet total cross section

$$\sigma_{np}{}^{(t)}=\frac{4\pi}{k^2}\sum_J\frac{2J+1}{3}(\sin^2\delta_J{}^\alpha+\sin^2\delta_J{}^\beta+\sin^2\delta_J{}^\gamma).\tag{60}$$

The triplet differential and total cross sections for tensor forces are completely analogous to the well-known formulas for central forces.[18] The differential cross section contains the phase shifts and the amounts of admixture, the total cross section contains the phase shifts only. In the following section we will derive these quantities from a variational principle.

C. Variational Principle for Phase Shifts

We start with the formal solutions (48), and consider first the phase shifts $\delta_J{}^\beta$ of the uncoupled states. Multiplication of the third equation by

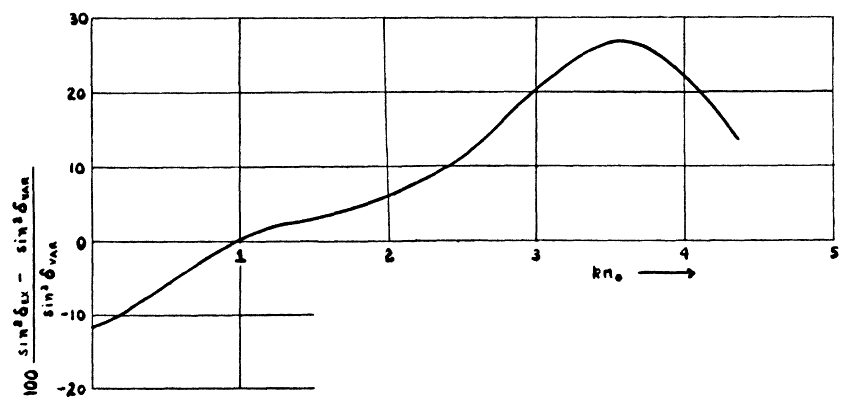

FIG. 6. Comparison of phase shifts: exact and variational calculations.

[30b] The dependence on m of these constants permits one to assume the boundary conditions (46′) with $\delta_J{}^\alpha$ and $\delta_J{}^\gamma$ independent of m.

$l(x)v_J(x)$ and integration leads readily to

$$-\cot\delta_J{}^\beta=\frac{\int l(x)v_J{}^2(x)dx+f\lambda\int l(x)v_J(x)dxG_J{}^v(x,x')dx'l(x')v_J(x')}{f\lambda\kappa\left(\int j_J(\kappa x)l(x)v_J(x)xdx\right)^2}, \qquad (61)$$

which is easily seen to be stationary with respect to variations of the radial function $v_J(x)$. The resulting phase shift will have an error of the second order for any first order error in a trial function $\bar{v}_J(x)$.

In a similar way the phase shifts for coupled states are obtained. Multiplication of the first Eq. (48) by $f_J(x)u_J(x)+g_J(x)w_J(x)$, and of the second by $g_J(x)u_J(x)+h_J(x)w_J(x)$, addition and integration yields because of $\delta_J{}^u=\delta_J{}^w=\delta_J$,

$$-\cot\delta_J=(a_J+2b_J+c_J)/(\alpha_J+2\beta_J+\gamma_J), \qquad (62)$$

where we used the following abbreviations:

$$a_J=(1/f\lambda)\int h_Jw_J{}^2dx+\int g_Jw_JdxG_J{}^udx'g_Jw_J+\int h_Jw_JdxG_J{}^wdx'h_Jw_J,$$

$$b_J=(1/f\lambda)\int g_Ju_Jw_Jdx+\int f_Ju_JdxG_J{}^udx'g_Jw_J+\int h_Jw_JdxG_J{}^wdx'g_Ju_J,$$

$$c_J=(1/f\lambda)\int f_Ju_J{}^2dx+\int g_Ju_JdxG_J{}^wdx'g_Ju_J+\int f_Ju_JdxG_J{}^udx'f_Ju_J \qquad (63)$$

$$\alpha_J=\kappa\left(\int xj_{J-1}(\kappa x)g_Jw_Jdx\right)^2+\kappa\left(\int xj_{J+1}(\kappa x)h_Jw_Jdx\right)^2,$$

$$\beta_J=\kappa\left(\int xj_{J-1}(\kappa x)f_Ju_Jdx\right)\left(\int xj_{J-1}g_Jw_Jdx\right)+\kappa\left(\int xj_{J+1}g_Ju_Jdx\right)\times\left(\int xj_{J+1}h_Jw_Jdx\right),$$

$$\gamma_J=\kappa\left(\int xj_{J-1}(\kappa x)f_Ju_Jdx\right)^2+\kappa\left(\int xj_{J+1}(\kappa x)g_Ju_Jdx\right)^2.$$

The expression (62) for $\cot\delta_J$ is stationary with respect to variations of $u_J(x)$ and $w_J(x)$. Both variational principles, (61) and (62), were first given by Schwinger.[11]

Equation (62) is homogeneous in $u_J(x)$ and $w_J(x)$, i.e., it depends only on the ratio of any constant factors multiplying these functions. Suppose we choose trial functions $\bar{u}_J(x)$ and $\xi_J\bar{w}_J(x)$, where ξ_J is a yet undetermined constant. The integrals (63) can then be evaluated with $\bar{u}_J(x)$ and $\bar{w}_J(x)$ replacing $u_J(x)$ and $w_J(x)$, respectively, and one finds from (62)

$$-\cot\delta_J=(\xi_J{}^2\bar{a}_J+2\xi_J\bar{b}_J+\bar{c}_J)/(\xi_J{}^2\bar{\alpha}_J+2\xi_J\bar{\beta}_J+\bar{\gamma}_J). \qquad (62')$$

TABLE XIIIa. Triplet phase shifts and amounts of admixture at 15.3 Mev. (Tensor forces, rectangular well, variational calculation of coupled phases.)

J		$\delta_J{}^\alpha$	$\delta_J{}^\beta$	$\delta_J{}^\gamma$	$\eta_J{}^\alpha$
	neutral			−0.1030	
0	charged			0.5378	—
	symmetric			0.0751	
	neutral		1.008		
1	charged	−1.4129	0.1153	0.0086	0.0712
	symmetric		−0.0549		
	neutral	0.1390		−0.0004	0.0600
2	charged	−0.0200	0.0145	0.0015	0.2645
	symmetric	−0.0142		0.0002	0.1259

TABLE XIIIb. Triplet phase shifts and amounts of admixture at 100 Mev. (Tensor forces, rectangular well, variational calculation of coupled phases.)

J		δ_J^α	δ_J^β	δ_J^γ	η_J^α
0	neutral charged symmetric			−0.6567 0.8450 0.3024	0
1	neutral charged symmetric	0.4031	0.9795 −0.7428 −0.3222	−0.1794	0.1984
2	neutral charged symmetric	0.5820 −0.2196 −0.1118	0.6812	−0.0794 0.2231 0.0504	0.3320 0.9754 0.6478
3	neutral charged symmetric	0.1918	0.1071 −0.0555 −0.0221	−0.0147	0.3016
4	any		0.0098		

This expression has now to be stationary with respect to ξ_J. We find

$$\xi_J = -(\bar{\beta}_J \cot\delta_J + \bar{b}_J)/(\bar{\alpha}_J \cot\delta_J + \bar{a}_J). \quad (64)$$

From (62′) and (64)

$$(\bar{\alpha}_J\bar{\gamma}_J - \bar{\beta}_J^2)\cot^2\delta_J + (\bar{a}_J\bar{\gamma}_J + \bar{\alpha}_J\bar{c}_J - 2\bar{b}_J\bar{\beta}_J) \times\cot\delta_J + \bar{a}_J\bar{c}_J - \bar{b}_J^2 = 0. \quad (65)$$

The two solutions of this equation give the two phase shifts δ_J^α and δ_J^γ. The constants ξ_J^α and ξ_J^γ follow then from (64), and the amounts of admixture from (51) and (47), where one puts $\delta_J^u = \delta_J^w = \delta_J^{\alpha,\gamma}$ and replaces $u_J(x)$ and $w_J(x)$ by $\bar{u}_J(x)$ and $\xi_J^{\alpha,\gamma}\bar{w}_J(x)$. The identity (52) provides for a valuable check of the calculations.

We used this variational procedure to calculate the cross sections for a rectangular well with the constants of Rarita and Schwinger[8] at 15 and 100 Mev. The trial functions were those which correspond to the Born-approximation

$$\bar{u}_J(x) = \kappa x j_{J-1}(\kappa x), \quad \bar{v}_J(x) = \kappa x j_J(\kappa x), \quad \bar{w}_J(x) = \kappa x j_{J+1}(\kappa x). \quad (66)$$

These trial functions will give better results the higher the energy and the higher the value of J. In order to obtain an estimate of the error we calculated the phase shift for the S-state in the non-tensor case with these trial functions ($\bar{v}_0(x)$) and the variational principle (61). One finds

$$-\cot\delta_0 = \left(\frac{2\kappa}{f\lambda} - \frac{\cos^2\kappa}{\kappa}\right)/(1-j_0(2\kappa)) + j_1(2\kappa)/(1-j_0(2\kappa))^2. \quad (67)$$

The exact solution is

$$-\cot\delta_0 = \left(1 + \frac{\kappa'}{\kappa}\cot\kappa'\cot\kappa\right) \Big/ \left(\cot\kappa - \frac{\kappa'}{\kappa}\cot\kappa'\right). \quad (68)$$

Figure 6 shows how the results compare for the triplet state at various energies. The error vanishes near 10 Mev ($\kappa\sim1$) where the S-phase shift passes through $-90°$. It has a maximum near 130 Mev ($\kappa\sim3.5$) and decreases for higher energies as expected. The variational value of $|\delta_0|$ is always larger than the exact value, and, therefore, the difference of the squares of $\sin\delta_0$ has to change sign near $-90°$. The small error below 40 Mev ($\kappa\sim2$) is due to the fact that the first term of the expansion of the trial function with respect to κx becomes more and more important, and that this term is the same as in the exact solution. At zero energy the exact and variational phase shifts are zero, and the function plotted in Fig. 6 becomes indeterminate; it approaches the finite limit -11.37 percent.

A great number of the integrals (63) could be evaluated analytically, when the trial functions (66) were used. The results for the phase shifts and the amounts of admixture for n-p scattering at 15 and 100 Mev are shown in Tables XIIIa and XIIIb. Since the phase shifts for the uncoupled states can also be found by the exact formulas (13) and (14), it is easy to find the error of the variational procedure. A comparison of the exact and the variational $^3P_0$ and $^3P_1$ phases is made in Table XIV.

The singlet, triplet, and total cross sections at 15 and 100 Mev for n-p scattering are tabulated in Table XV. The cross sections at 100 Mev for n-n scattering are given in Table XVI.

Since the partial wave $\psi_{1,m}^\alpha$ is mainly an S-state as can be seen from the amounts of admixture, we will expect its contribution to the triplet

TABLE XIV. Comparison of P-phases.

Energy Mev	Theory	$^3P_0$ Exact	$^3P_0$ Var.	$^3P_1$ Exact	$^3P_1$ Var.
15.3	neutral charged symmetric	−0.1030 0.5378 0.07514	−0.1023 0.5104 0.07496	1.0081 0.1153 −0.05489	0.9151 0.1141 −0.05483
100.3	neutral charged symmetric	−0.6567 0.8450 0.3024	−0.6422 0.8149 0.3009	0.9795 −0.7428 −0.3222	0.9328 −0.7219 −0.3205

cross sections to be off the exact value by about the same amount as the S-state of the corresponding non-tensor case (Fig. 6). For 15 Mev ($\kappa \sim 1.2$) and 100 Mev ($\kappa = 3.08$) this error is 2 percent and 22 percent, respectively. It amounts to a maximum correction of 0.01 barn and 0.0025 barn for the total cross sections at these two energies (Table XV). The total cross sections at 15.3 Mev are in excellent agreement with the exact calculations of Rarita and Schwinger[8] which obtained 0.621, 0.666, and 0.983 barn for the symmetrical, charged, and neutral theory, respectively. Exact calculations at 100 Mev by Ashkin and Wu[10] give 0.129 barn for the total n-p cross section which is to be compared with our value of 0.1271(+0.0025 max.) barn of the symmetrical theory. All three theories give n-p cross sections at 100 Mev which compare well with the calculations at 83 Mev of Massey, Burhop, and Hu,[15] namely 0.1410, 0.1577, and 0.2388 barn for the symmetrical, charged, and neutral theory, respectively.

CONCLUSIONS

Recent experiments[5, 6a] on neutron-proton scattering at 90 Mev gave a cross section $\sigma_{np} = 0.083 \pm 0.004$ barn. The angular distribution in the center of mass system seems to be symmetrical around 90° and yields a ratio $R = \sigma_{np}(\pi)/\sigma_{np}(\pi/2)$ of about 3. None of the phenomenological theories discussed so far in this paper yield these results. Qualitatively, the neutral theory is ruled out, because it leads to $R < 1$; the charged theory leads to too large values of R; closest to the observations comes the symmetrical theory. The non-tensor theory leads to practically no sideward scattering, in contradiction to the experiments. A large increase of $\sigma(\pi/2)$ is obtained by the addition of a tensor part to the potential (compare Fig. 1 with Figs. 4 and 5.)

At 100 Mev in the symmetrical theory, the tensor force increases the total cross section for a rectangular well, but decreases it for a Yukawa well. The latter yields $\sigma_{np}(\text{Born}) = 0.089$ barn with the better set of constants (Table X); the exact value may be larger by an error of the order of 5 percent. The Born approximation value of R is three times too large. A decrease of the tensor range could sufficiently decrease the total cross section and would make the angular distribution more isotropic. On the other hand, a relativistic correction would have to account for a decrease in the total cross section by 5–10 percent; this is not impossible.[6b] It would also have to account for a large decrease of R. *We conclude, that the symmetrical tensor theory with a Yukawa well may be in agreement with the experiments, if the relativistic corrections at 100 Mev are taken into account and the tensor range is reduced.*

Under the assumption that the symmetry of the angular distribution around 90° can be experimentally established, a new type of exchange force suggests itself. It would consist of equal amounts of neutral and charged exchange potential, such that only even states contribute to the cross section.[31] The exchange operator in (28) would be in this case, as follows from (33),

$$f(\sigma_1\cdot\sigma_2,\, \tau_1\cdot\tau_2) = -\frac{1}{2}\left(1 - \frac{1+\sigma_1\cdot\sigma_2}{2}\,\frac{1+\tau_1\cdot\tau_2}{2}\right) = -\tfrac{1}{2}(1+(-1)^L). \quad (69)$$

From our exact and variational calculations we find for a rectangular well of ranges 2.80×10^{-13} cm the n-p cross sections at 100 Mev as shown in Table XVII. The total tensor cross section

TABLE XV. Cross sections for n-p scattering at 15 and 100 Mev. (Tensor forces, rectangular well potential, variational calculation of phases.)

Theory	15 Mev $\sigma_{np}^{(s)}$	15 Mev $\sigma_{np}^{(t)}$	15 Mev σ_{np}	100 Mev $\sigma_{np}^{(s)}$	100 Mev $\sigma_{np}^{(t)}$	100 Mev σ_{np}
Neutral	0.4369	1.1145	0.9833	0.06455	0.2602	0.2113
Charged	0.4236	0.7262	0.6657	0.05523	0.1812	0.1497
Symmetric	0.4445	0.6663	0.6108	0.16916	0.1131	0.1271

TABLE XVI. Cross sections for n-n scattering at 100 Mev. (Tensor forces, rectangular well, variational calculation of coupled states.)

	$\sigma_{nn}^{(s)}$	$\sigma_{nn}^{(t)}$	σ_{nn}
Neutral	0.04636	0.32661	0.25655
Charged	0.04636	0.16864	0.13807
Symmetric	0.04636	0.03239	0.03588

TABLE XVII. Neutron-proton cross sections at 100 Mev for an even interaction potential. (Rectangular well, phase method.)

Force	$\sigma_{np}^{(s)}$	$\sigma_{np}^{(t)}$	σ_{np}
Central	0.02318	0.06543	0.05487
Tensor	0.02318	0.09688	0.07831

[31] Ashkin and Wu (reference 10) quote Serber on this point.

may again be too small by less or about 0.0025 barn. Since the odd states do not contribute much to the scattering at 90°, the differential cross section at this angle will be not much smaller than in the symmetrical tensor theory, where the odd states are reduced to one third in their potential. This will be close to the observed value. From the symmetry and the strongly reduced total cross section it then follows that R will be much smaller than in the symmetrical tensor theory.

Two neutrons interact only in odd triplet and even singlet states. With the exchange force (69) they will interact only in singlet states. We find from (22): $\sigma_{nn}=2\sigma_{np}^{(s)}=0.04636$ barn. The symmetrical tensor theory gives (Table XV) $\sigma_{nn}=0.03588$ barn. The experimental value of the difference between the n-d and the n-p cross section at 90 Mev is[6a] 0.034±0.003 barn. However, Wu and Ashkin[32] have shown that the n-n cross section may be appreciably larger than this difference. Therefore, either theory can be correct.

Finally, one should mention that a potential of the exchange type (69) is also in agreement with the measurements of Laughlin and Kruger.[4] The ratio $R=1.05$ which follows from the calculations of Rarita and Schwinger[8] for 15 Mev is certainly within the experimental error.

We conclude, therefore, that, *if relativistic corrections at 100 Mev are negligible, the scattering experiments are consistent with a nucleon tensor force which acts only in even states.*

ACKNOWLEDGMENT

We are grateful to Professor Julian Schwinger for helpful discussions of many aspects of this problem. One of us (F. R.) would also like to acknowledge the support he has received during this work from a Bayard Cutting Fellowship for Research in Physics.

APPENDIX: FORMULAS FOR THE DIFFERENTIAL AND TOTAL CROSS SECTIONS

A. Born Approximation

a. N-P Cross Sections

With the notation used in this paper and the symbols

$$\xi=2\kappa\sin\vartheta/2,\quad \chi=2\kappa\cos\vartheta/2;$$

the cross sections are found to have the following convenient forms:

For central forces and a rectangular well:

Differential cross section,

neutral:
$$\sigma_{np}(\vartheta)=\lambda^2 r_0^2 j_1^2(\xi)/\xi^2 \quad \text{(singlet or triplet)}, \tag{A2}$$

charged:
$$\sigma_{np}(\vartheta)=\lambda^2 r_0^2 j_1^2(\chi)/\chi^2 \quad \text{(singlet or triplet)}, \tag{A3}$$

symmetric:
$$\sigma_{np}^{(s)}(\vartheta)=\lambda_s^2 r_0^2[j_1(\xi)/\xi-2j_1(\chi)/\chi]^2, \tag{A4}$$
$$\sigma_{np}^{(t)}(\vartheta)=\lambda_t^2 r_0^2[j_1(\xi)/\xi+2j_1(\chi)/\chi]^2. \tag{A5}$$

Total cross section,

neutral and charged:
$$\sigma_{np}=\frac{\pi}{2k^2}\lambda^2[1-j_0^2(2\kappa)-j_1^2(2\kappa)] \quad \text{(singlet or triplet)}, \tag{A6}$$

symmetric:
$$\sigma_{np}^{(s)}=\frac{2\pi}{k^2}\lambda_s^2\{(5/4)[1-j_0^2(2\kappa)-j_1^2(2\kappa)]-R_0(\kappa)\}, \tag{A7}$$
$$\sigma_{np}^{(t)}=\frac{1}{9}\frac{2\pi}{k^2}\lambda_t^2\{(5/4)[1-j_0^2(2\kappa)-j_1^2(2\kappa)]+R_0(\kappa)\}, \tag{A8}$$

where

$$R_0(\kappa)=\int_0^\pi j_1(\xi)j_1(\chi)d\vartheta =\kappa^2\sum_{L=0}^{\infty}(-1)^L(2L+1)[j_L^2(\kappa)-j_{L-1}(\kappa)j_{L+1}(\kappa)]. \tag{A9}$$

For central forces and a Yukawa well:

neutral:
$$\sigma_{np}(\vartheta)=\lambda^2 r_y^2/(1+\xi^2)^2 \quad \text{(singlet or triplet)}, \tag{A10}$$

charged:
$$\sigma_{np}(\vartheta)=\lambda^2 r_y^2/(1+\chi^2)^2 \quad \text{(singlet or triplet)}, \tag{A11}$$

symmetric:
$$\sigma_{np}^{(s)}(\vartheta)=\lambda_s^2 r_y^2[1/(1+\xi^2)^2-2/(1+\chi^2)^2], \tag{A12}$$
$$\sigma_{np}^{(t)}(\vartheta)=\tfrac{1}{9}\lambda_t^2 r_y^2[1/(1+\xi^2)^2+2/(1+\chi^2)^2]. \tag{A13}$$

Total cross section,

neutral and charged:
$$\sigma_{np}=\frac{\pi}{k^2}\lambda^2(2\kappa)^2/[1+(2\kappa)^2] \quad \text{(singlet or triplet)}, \tag{A14}$$

symmetric:
$$\sigma_{np}^{(s)}=\frac{\pi}{k^2}\lambda_s^2\left[5\frac{(2\kappa)^2}{1+(2\kappa)^2}-\frac{4}{1+2\kappa^2}\ln[1+(2\kappa)^2]\right], \tag{A15}$$
$$\sigma_{np}^{(t)}=\frac{1}{9}\frac{\pi}{k^2}\lambda_t^2\left[5\frac{(2\kappa)^2}{1+(2\kappa)^2}+\frac{4}{1+2\kappa^2}\ln[1+(2\kappa)^2]\right]. \tag{A16}$$

For tensor forces and a rectangular well:

Differential cross section,

neutral
$$\sigma_{np}^{(t)}=\lambda_t^2 r_0^2[j_1^2(\xi)/\xi^2+8\gamma^2 r_2^2(\xi)], \tag{A17}$$

[32] T. Y. Wu and J. Ashkin, Phys. Rev. **73**, 986 (1948).

charged: same with ξ replaced by χ.
symmetric:

$$\sigma_{np}^{(t)}=\tfrac{1}{9}\lambda_t^2 r_0^2\{[j_1(\xi)/\xi+2j_1(\chi)/\chi]^2+8\gamma^2[r_2^2(\xi)-2r_2(\xi)r_2(\chi)+4r_2^2(\chi)]\},\quad (A18)$$

where

$$r_2(\xi)=\int_0^1 j_2(\xi x)x^2dx=(3Si\xi-4\sin\xi+\xi\cos\xi)/\xi^3.\quad (A19)$$

Total cross section,
neutral and charged:

$$\sigma_{np}^{(t)}=\frac{\pi}{k^2}\lambda_t^2\{\tfrac{1}{2}[1-j_0^2(2\kappa)-j_1^2(2\kappa)]+8\gamma^2R_2(2\kappa)\},\quad (A20)$$

symmetric:

$$\sigma_{np}^{(t)}=\frac{1}{9}\frac{2\pi}{k^2}\lambda_t^2\left\{\frac{5}{4}[1-j_0^2(2\kappa)-j_1^2(2\kappa)]+R_0(\kappa)+8\gamma^2\left[5R_2(2\kappa)-\int_0^\pi r_2(\xi)r_2(\chi)\xi\chi d\vartheta\right]\right\},\quad (A21)$$

where

$$R_2(2\kappa)=\int_0^{2\kappa} r_2^2(\xi)\xi d\xi.\quad (A22)$$

The integral over the cross term and the integral $R_2(2\kappa)$ of (A22) can be evaluated analytically, but the resulting expressions are too complicated to be given here.

For tensor forces and a Yukawa well:
Differential cross section,
neutral:

$$\sigma_{np}^{(t)}=\lambda_t^2 r_y^2[1/(1+\xi^2)^2+8\gamma^2y_2^2(\xi)],\quad (A23)$$

charged: same with ξ replaced by χ.
symmetric:

$$\sigma_{np}^{(t)}=\tfrac{1}{9}\lambda_t^2 r_y^2\{[1/(1+\xi^2)+2/(1+\chi^2)]^2+16\gamma^2[y_2^2(\xi)-2y_2(\xi)y_2(\chi)+4y_2^2(\chi)]\},\quad (A24)$$

where

$$y_2(\xi)=\int_0^\infty j_2(\xi x)e^{-x}xdx=\frac{3}{\xi^2}(1-\tan^{-1}\xi/\xi)-1/(1+\xi^2),\quad (A25)$$

Total cross section,
neutral and charged:

$$\sigma_{np}^{(t)}=\frac{\pi}{k^2}\lambda_t^2\left[\frac{(2\kappa)^2}{1+(2\kappa)^2}+16\gamma^2Y_2(2\kappa)\right],\quad (A26)$$

symmetric:

$$\sigma_{np}^{(t)}=\frac{1}{9}\frac{\pi}{k^2}\lambda_t^2\left\{5\frac{(2\kappa)^2}{1+(2\kappa)^2}+\frac{4}{1+2\kappa^2}\ln[1+(2\kappa)^2]+16\gamma^2\left[5Y_2(2\kappa)-\int_0^\pi y_2(\xi)y_2(\chi)\xi\chi d\vartheta\right]\right\},\quad (A27)$$

where

$$Y_2(2\kappa)=\int_0^{2\kappa} y_2^2(\xi)\xi d\xi=2-\tfrac{1}{2}1/[1+(2\kappa)^2]-(9/4)1/(2\kappa)^2-\tfrac{3}{4}(\tan^{-1}2\kappa)^2(1+3/(2\kappa)^4)-\tfrac{3}{2}\tan^{-1}2\kappa(1-3/(2\kappa)^2)/2\kappa.\quad (A28)$$

b. N-N Cross Section

The singlet cross section is the same for all exchange theories, central or tensor forces. It is for a rectangular well

$$\sigma_{nn}^{(s)}(\vartheta)=\lambda_s^2r_0^2[j_1(\xi)/\xi+j_1(\chi)/\chi]^2,\quad (A29)$$

$$\sigma_{nn}^{(s)}=\frac{\pi}{2k^2}\lambda_s^2[1-j_0^2(2\kappa)-j_1^2(2\kappa)+2R_0(\kappa)],\quad (A30)$$

and for a Yukawa well

$$\sigma_{nn}^{(s)}(\vartheta)=\lambda_s^2r_y^2[1/(1+\xi^2)+1/(1+\chi^2)],\quad (A31)$$

$$\sigma_{nn}^{(s)}=\frac{\pi}{k^2}\lambda_s^2\left[\frac{(2\kappa)^2}{1+(2\kappa)^2}+\frac{1}{1+2\kappa^2}\ln[1+(2\kappa)^2]\right].\quad (A32)$$

The triplet cross section in the charged theory is the same as in the neutral theory, and in the symmetrical theory it is $\frac{1}{9}$th of that in the neutral theory. The neutral triplet cross section is—

for central forces and a rectangular well:

$$\sigma_{nn}^{(t)}(\vartheta)=\lambda_t^2r_0^2[j_1(\xi)/\xi-j_1(\chi)/\chi]^2,\quad (A33)$$

$$\sigma_{nn}^{(t)}=\frac{\pi}{2k^2}\lambda_t^2[1-j_0^2(2\kappa)-j_1^2(2\kappa)-2R_0(\kappa)],\quad (A34)$$

for central forces and a Yukawa well:

$$\sigma_{nn}^{(t)}(\vartheta)=\lambda_t^2r_y^2[1/(1+\xi^2)-1/(1+\chi^2)]^2,\quad (A35)$$

$$\sigma_{nn}^{(t)}=\frac{\pi}{k^2}\lambda_t^2\left[\frac{(2\kappa)^2}{1+(2\kappa)^2}-\frac{1}{1+2\kappa^2}\ln[1+(2\kappa)^2]\right];\quad (A36)$$

for tensor forces and a rectangular well:

$$\sigma_{nn}^{(t)}(\vartheta)=\lambda_t^2r_0^2\{[j_1(\xi)/\xi-j_1(\chi)/\chi]^2+8\gamma^2[r_2^2(\xi)+r_2(\xi)r_2(\chi)+r_2^2(\chi)]\},\quad (A37)$$

$$\sigma_{nn}^{(t)}=\frac{\pi}{2k^2}\lambda_t^2\left\{1-j_0^2(2\kappa)-j_1^2(2\kappa)-2R_0(\kappa)+8\gamma^2\left[4R_2(2\kappa)+\int_0^\pi r_2(\xi)r_2(\chi)\xi\chi d\vartheta\right]\right\},\quad (A38)$$

where R_0, r_2, and R_2 are defined in (A9), (A19), and (A22);

for tensor forces and a Yukawa well:

$$\sigma_{nn}^{(t)}(\vartheta)=\lambda_t^2r_y^2\{[1/(1+\xi^2)-1/(1+\chi^2)]^2+8\gamma^2[y_2^2(\xi)+y_2(\xi)y_2(\chi)+y_2^2(\chi)]\},\quad (A39)$$

$$\sigma_{nn}^{(t)}=\frac{\pi}{k^2}\lambda_t^2\left\{\frac{(2\kappa)^2}{1+(2\kappa)^2}+\frac{1}{1+2\kappa^2}\ln[1+(2\kappa)^2]+8\gamma^2\left[2Y_2(2\kappa)+\frac{1}{2}\int_0^\pi y_2(\xi)y_2(\chi)\xi\chi d\vartheta\right]\right\},\quad (A40)$$

where y_2 and Y_2 are defined in (A25) and in (A28).

B. Phase Method for Tensor Forces

The differential cross section (59) can be written

$$\sigma^{(t)}(\vartheta)=\frac{1}{k^2}\sum_n c_n \cos^n\vartheta. \tag{A41}$$

When all the S, P, and D states are taken into account, but the coupling to higher angular momenta is neglected, one obtains for n-p scattering

$$\begin{aligned}
c_0=&\frac{1}{3}({}^3P_0)+\left(1-\frac{\left(1+\frac{1}{(8)^{\frac12}}e^{-\zeta_1}\right)^2}{2\cosh^2\zeta_1}\right)({}^3S_1)\\
&+\frac{3}{4}({}^3P_1)+\frac{13}{12}({}^3P_2)+\left(1-\frac{\left(1-\frac{1}{(8)^{\frac12}}e^{\zeta_1}\right)^2}{2\cosh^2\zeta_1}\right)({}^3D_1)\\
&+\frac{25}{12}({}^3D_2)+\frac{19}{12}({}^3D_3)-\frac{(\sinh\zeta_1+1/(8)^{\frac12})^2}{2\cosh^2\zeta_1}\\
&\times({}^3S_1+{}^3D_1)-\frac{1}{3}({}^3P_0+{}^3P_2)-\frac{3}{4}({}^3P_1+{}^3P_2)\\
&+\frac{5}{12}({}^3D_2+{}^3D_3)-\frac{5e^{\zeta_1}(1+\sqrt{2}e^{-\zeta_1})^2}{24\cosh\zeta_1}({}^3D_1+{}^3D_2)\\
&+\frac{-\frac{7}{6}e^{\zeta_1}-\frac{\sqrt{2}}{12}+\frac{11}{12}e^{-\zeta_1}}{2\cosh\zeta_1}({}^3S_1+{}^3D_1)\\
&-\frac{5e^{-\zeta_1}(1-\sqrt{2}e^{\zeta_1})^2}{24\cosh\zeta_1}({}^3S_1+{}^3D_2),\\
c_1=&\frac{e^{-\zeta_1}(e^{\zeta_1}+\sqrt{2})^2}{6\cosh\zeta_1}({}^3S_1+{}^3P_0)+\frac{e^{-\zeta_1}(1-\sqrt{2}e^{\zeta_1})^2}{4\cosh\zeta_1}\\
&\times({}^3S_1+{}^3P_1)+\frac{10e^{\zeta_1}-16e^{-\zeta_1}}{12\cosh\zeta_1}({}^3S_1+{}^3P_2)\\
&+\frac{e^{\zeta_1}(e^{-\zeta_1}-\sqrt{2})^2}{6\cosh\zeta_1}({}^3P_0+{}^3D_1)-\frac{3}{2}({}^3P_0+{}^3D_3)\\
&+\frac{e^{\zeta_1}(1+\sqrt{2}e^{-\zeta_1})^2}{4\cosh\zeta_1}({}^3P_1+{}^3D_1)-3({}^3P_1+{}^3D_3)\\
&+\frac{5e^{-\zeta_1}-8e^{\zeta_1}}{6\cosh\zeta_1}({}^3P_2+{}^3D_1)-\frac{5}{2}({}^3P_2+{}^3D_2)\\
&+({}^3P_2+{}^3D_2),
\end{aligned} \tag{A42}$$

$$\begin{aligned}
c_2=&\frac{3}{2}\frac{\left(1+\frac{1}{(8)^{\frac12}}e^{-\zeta_1}\right)^2}{\cosh^2\zeta_1}({}^3S_1)+\frac{3}{4}({}^3p_1)\\
&+\frac{3}{2}\frac{\left(1-\frac{1}{(8)^{\frac12}}e^{\zeta_1}\right)^2}{\cosh^2\zeta_1}({}^3D_1)+\frac{7}{4}({}^3P_2)-\frac{25}{4}({}^3D_2)\\
&-\frac{1}{2}({}^3D_3)+\frac{3}{2}\frac{(\sin\zeta_1+1/(8)^{\frac12})^2}{\cosh^2\zeta_1}({}^3S_1+{}^3D_1)\\
&+({}^3P_0+{}^3P_2)+\frac{9}{4}({}^3P_1+{}^3P_2)-\frac{15}{2}({}^3D_2+{}^3D_3)\\
&+\frac{5}{8}\frac{e^{\zeta_1}(1+\sqrt{2}e^{-\zeta_1})^2}{\cosh\zeta_1}({}^3D_1+{}^3D_2)\\
&+\frac{\frac{7}{2}e^{-\zeta_1}-\sqrt{2}-\frac{19}{2}e^{\zeta_1}}{2\cosh\zeta_1}({}^3D_1+{}^3D_3)\\
&+\frac{5}{8}\frac{e^{-\zeta_1}(1-\sqrt{2}e^{\zeta_1})^2}{\cosh\zeta_1}({}^3S_1+{}^3D_3)\\
&+\frac{\frac{7}{2}e^{\zeta_1}+\sqrt{2}-\frac{19}{2}e^{-\zeta_1}}{2\cosh\zeta_1}({}^3S_1+{}^3D_3),\\
c_3=&\frac{9e^{-\zeta_1}}{4\cosh\zeta_1}({}^3S_1+{}^3P_2)+\frac{5}{2}({}^3P_0+{}^3D_3)+\frac{5}{2}({}^3P_1+{}^3D_2)\\
&+5({}^3P_1+{}^3D_3)+\frac{9e^{\zeta_1}}{4\cosh\zeta_1}({}^3P_2+{}^3D_1)\\
&+5({}^3P_2+{}^3D_2)+3({}^3P_2+{}^3D_3)\},\\
c_4=&\frac{25}{3}({}^3D_2)+\frac{55}{12}({}^3D_3)+\frac{125}{12}({}^3D_2+{}^3D_3)\\
&+\frac{45e^{\zeta_1}}{8\cosh\zeta_1}({}^3D_1+{}^3D_3)+\frac{45e^{-\zeta_1}}{8\cosh\zeta_1}({}^3S_1+{}^3D_3),
\end{aligned}$$

where

$$\begin{aligned}
&\zeta_1=-\ln\eta_1{}^{\alpha},\\
&({}^3L_J)=\sin^2\delta_J{}^{\alpha,\beta,\gamma}\quad \begin{matrix}\alpha\rightarrow L=J-1\\ \beta\rightarrow L=J\\ \gamma\rightarrow L=J+1\end{matrix},\\
&({}^3L_J+{}^3L'_{J'})=2\sin\delta_J{}^{\alpha,\beta,\gamma}\sin\delta_{J'}{}^{\alpha',\beta',\gamma'}\cos(\delta_J-\delta_{J'}).
\end{aligned} \tag{A43}$$

The n-n cross section is obtained from this by omission of all the even phases and multiplication by a factor of four.